Bull. Mater. Sci. (2020) 43:103
https://doi.org/10.1007/s12034-020-2082-z

Effect of carbon on structural and magnetic properties of $Ge_{1-x}Mn_x$ nanocolumns

T G LE[1,*], V LE THANH[2] and L MICHEZ[2]

[1]Department of Engineering and Technology, Hong Duc University, 40130 Thanh Hoa City, Vietnam
[2]Interdisciplinary Center of Nanoscience of Marseille (CINaM-CNRS), Aix-Marseille University, Campus of Luminy, Case 913, 13288 Marseille, France
*Author for correspondence (lethigiang@hdu.edu.vn)

MS received 16 August 2019; accepted 24 December 2019

Abstract. We have investigated the structural and magnetic properties of $Ge_{0.94}Mn_{0.06-\delta}C_\delta$ films ($\delta = 0.005$, 0.01 and 0.02) using reflexion high-energy electron diffraction (RHEED) technique, transmission electron microscopy (TEM) and superconducting quantum interference device magnetometer. All films have been prepared by co-depositing Ge, Mn and C by molecular beam epitaxy. RHEED pattern shows the increase in sample surface roughness when doping carbon into the GeMn films. TEM analyses indicate that adding carbon greatly reduces the surface diffusion of both Ge and Mn elements. Ferromagnetic ordering in samples containing carbon contents of 0.01 and 0.02, persists at temperatures >400 K. An increase in net magnetization is found for carbon-doped samples with increasing carbon content from 0.01 to 0.02. However, we found a decrease in the net magnetization and the Curie temperature of the samples after annealing at 450 and 650°C. The Curie temperature reduces down to about 300 K, which is comparable to the value of the free-carbon sample showing a harmful effect of the post-annealing on the magnetic properties of carbon-doped GeMn nanocolumns.

Keywords. GeMn nanocolumns; Mn_5Ge_3; carbon doping; GeMn magnetization; thermal stability.

1. Introduction

GeMn-based diluted magnetic semiconductor have attracted great interest for applications in the field of semiconductor spintronics [1–6]. At the growth conditions far from thermodynamic equilibrium and in the temperature range between 110 and 150°C, the materials possess the GeMn-nanocolumnar structure with the Curie temperature (T_c) >400 K [1,7–9]. They exhibit a dilute magnetic semiconductor-like metastable single crystalline Ge structure without precipitation of ferromagnetic intermetallic $Ge_{1-x}Mn_x$ or GeMn amorphous phases.

For the $Ge_{1-x}Mn_x$ nanocolumns showing $T_c > 400$ K, one may foresee a high potential in fabrication of nano-devices, such as memory nanodots or nanochannels for emerging spin-related transport. In fact, the $Ge_{1-x}Mn_x$ nanocolumns are a meta-stable phase. In the work of Jamet *et al* [1], the nanocolumns remain stable up to 400°C during annealing under ultrahigh-vacuum conditions. However, 15-min annealing at 650°C activates a volume diffusion of Mn atoms, and the nanocolumns collapse into Mn_5Ge_3 nanoparticles with their average diameter of about 10–12 nm [1,7]. In view of the device fabrication, an important property of materials that should be controlled is their thermal stability. In general, it is desirable that materials remain stable up to temperatures >700°C, since in device fabrication processes, thermal annealing is needed, in particular, for the dopant implantation and the deposition of metallic and dielectric layers. Therefore, an approach that allows to thermally stabilize the $Ge_{1-x}Mn_x$ nanocolumnar phase represents a particular interest for spintronic applications.

It has been shown that when doping the Mn_5Ge_3 compound with carbon, carbon atoms can be incorporated into interstitial sites of the Mn_5Ge_3 lattice due to its small atomic radius and greatly reduce Ge and Mn inter-diffusion [10,11]. Resulting compound, $Mn_5Ge_3C_x$, can be stable up to a temperature >850°C, as compared to 650°C of a carbon-free Mn_5Ge_3 layer. In addition, it has been demonstrated from both theoretical [12] and experimental studies [10,11] that the magnetic properties of the carbon-doped $Mn_5Ge_3C_x$ compound may be tuned, thanks to the enhanced coupling interactions between neighbouring Mn atoms mediated by interstitial carbon. It has been also shown that adsorption of some monolayers of carbon on top of a Mn_5Ge_3 film can prevent from the out-diffusion of Mn from Mn_5Ge_3 [13,14]. As reported in our previous studies, in $Ge_{1-x}Mn_x$ nanocolumns, the Mn concentration is relatively high (up to ∼40%) and Mn atoms inside nanocolumns exhibit a tendency to segregate upwards the surface (increase of Mn concentration from the interface to the film surface) [15–17].

In this respect, the use of carbon is a promising approach to tune the magnetic properties and stabilize the structure

Published online: 01 April 2020

of $Ge_{1-x}Mn_x$ nanocolumns. This paper focusses on molecular beam epitaxy (MBE) growth of carbon-doped $Ge_{1-x}Mn_x$ nanocolumns and investigates the carbon effect on the structural and magnetic properties of the nanocolumns.

2. Experimental

Growth was performed using solid source MBE on epi-ready Ge(001) wafers with a residual n-type doping and resistivity of 10^{15} cm^{-3} and 10 Ω cm, respectively. Ge and Mn were evaporated using standard Knudsen effusion cells. The deposition rate (Ge) is about 0.2 Å s^{-1}. The deposition chamber is equipped with reflection high-energy electron diffraction (RHEED) to control the sample surface and to monitor the epitaxial growth process. The Ge deposition rate was estimated from RHEED intensity oscillations of the Ge-on-Ge homoepitaxy, whereas the Mn concentrations were deduced from Rutherford backscattering spectrometry (RBS) measurements.

To investigate the effect of carbon on the formation of $Ge_{1-x}Mn_x$ nanocolumns, we have added carbon with various concentrations during the co-deposition of Ge and Mn; the growth parameters (substrate temperature and Mn concentrations) were kept constant as those used for the growth of $Ge_{1-x}Mn_x$ nanocolumns [8,9]. Carbon evaporation was carried out based on the sublimation of the high purity pryolytic graphite (MBE-Komponenten Company). Post-annealing was carried out from 450 to 650°C in high vacuum and the annealing duration was 20 min to insure a complete phase transformation. The carbon concentration was estimated from the change of Si(001) surface reconstructions from (2×1) to c(4×4) upon adsorption of a carbon sub-monolayer [10–21].

Transmission electron microscopy (TEM) observations were performed using JEOL 3010 microscope with an acceleration voltage of 300 kV and a spatial resolution of 1.7 Å. Sample preparation was carried out by standard mechanical polishing and argon ion milling. The magnetic properties were characterized using superconducting quantum interference device (SQUID) magnetometer in the temperature range from 5 to 400 K with a magnetic field of 0.5 T applied parallel to the surface of the samples.

3. Results and discussion

To investigate the effect of carbon on the formation of nanocolumns, we have carried out a preliminary set of experiments, in which we first grew GeMn nanocolumns (free of carbon) for several thicknesses and then, added carbon with various concentrations during the co-deposition of Ge and Mn. The change in RHEED patterns upon carbon addition provided us a first signature of the carbon effect on the evolution of the surface morphology. Figure 1a displays a RHEED pattern, which is indicative of the characteristics of the surface of GeMn nanocolumns. The surface still exhibits a two-dimensional growth behaviour although some intensity reinforcements at the Bragg diffraction positions are visible and the intensity of reconstructed $\frac{1}{2}$ streaks becomes weaker—the fingerprint of the GeMn nanocolumn formation [9].

Upon carbon addition, the RHEED pattern is found to be spotty, indicating that the surface roughness increased. For a high carbon concentration, diffracted ring feature due to polycrystalline phase appears in RHEED patterns. We show in figure 1b, an example of a RHEED pattern corresponding to a carbon content $\delta = 0.005$. It can be seen that the RHEED pattern is mainly characterized by three-dimensional spots and rings.

Figure 2a shows the cross-sectional TEM image of a sample, in which a very small amount of carbon ($\delta \approx 0.005$) was added during the co-deposition of Ge and Mn on top of 20-nm thick layer of $Ge_{0.94}Mn_{0.06}$ nanocolumn. Dark contrast corresponds to Mn-rich regions, while regions with a brighter contrast arise from the diluted matrix. It can be seen that the

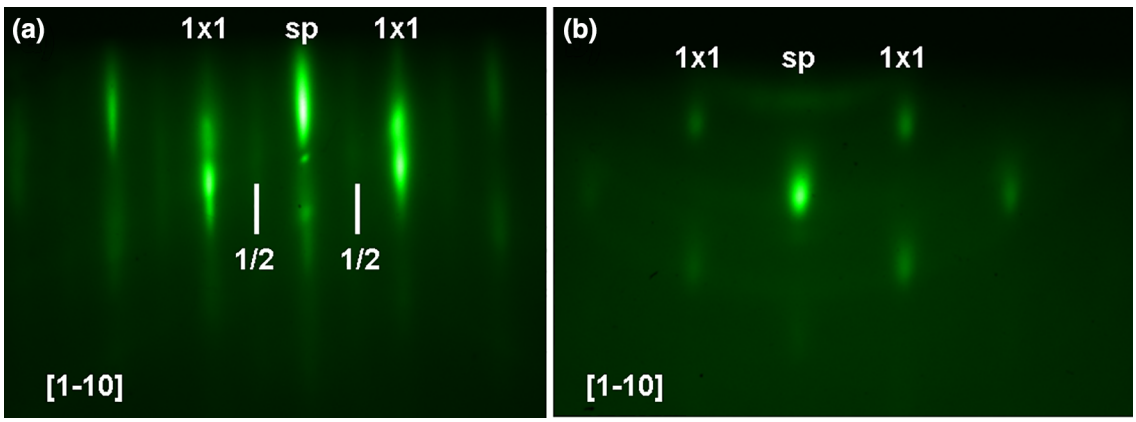

Figure 1. RHEED patterns taken along [1–10] azimuth (**a**) during the growth of carbon-free $Ge_{0.94}Mn_{0.06}$ nanocolumns and (**b**) during the $Ge_{0.94}Mn_{0.055}C_{0.005}$ growth.

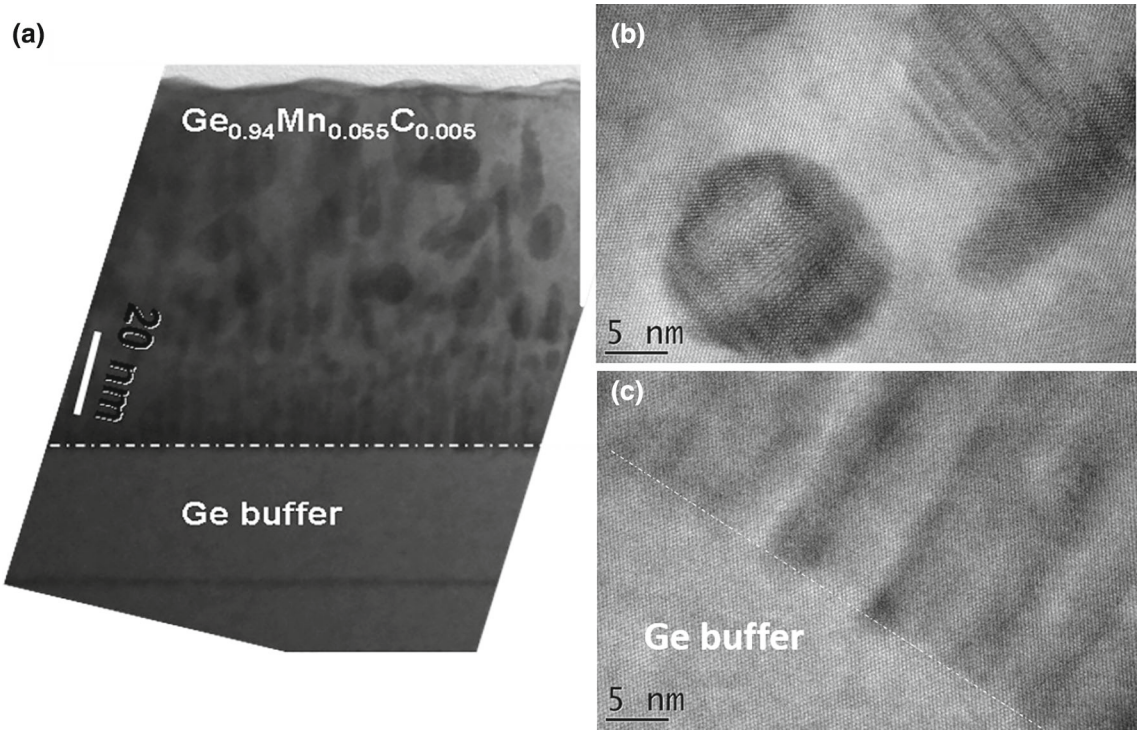

Figure 2. (**a**) Typical TEM image of ∼80-nm thick $Ge_{0.94}Mn_{0.055}C_{0.005}$; (**b**) high-resolution TEM micrographs of the $Ge_{0.94}Mn_{0.055}C_{0.005}$ film and (**c**) the region around the interface between Ge buffer and $Ge_{0.94}Mn_{0.06}$ film.

addition of carbon has disturbed the nanocolumn formation. The film has been divided into two distinct parts. Around the interface region (interface between the GeMn film and Ge buffer layers), nanocolumns appear to be dominant. However, in the upper part of the layer (about 60-nm thick), even some nanocolumns still exist, but they have a smaller length, a larger diameter and in particular, they are distributed in a disordered manner. As can be seen in a high-resolution TEM image taken around the interface region (figure 2c), most of nanocolumns are oriented perpendicular to the interface with the size of about 3–5 nm. Besides, MnGeC precipitates or clusters having a size >10 nm are found by high-resolution TEM micrographs of $Ge_{0.94}Mn_{0.06}C_{0.005}$ films shown in figure 2b. The results obtained from TEM images are in good agreement with the observation of the change in the RHEED patterns (the RHEED patterns change from fingerprint of the GeMn nanocolumn formation to mainly characterized by three-dimensional spots and rings due to polycrystalline phase appears when co-deposition of Ge, Mn and C).

To get insights into the evolution of the film structure upon carbon doping, we show in figure 3 that the TEM images of the samples with the carbon concentrations of 0.01 and 0.02. Carbon doping was carried out at the same time with Ge and Mn depositions. One can see that the GeMn nanocolumns are no longer formed, and the layers exhibit structures, which are less homogeneous and they become more disordered with increase in the carbon content. The TEM analyses clearly indicate that adding carbon greatly reduces the surface diffusion, probably of both the elements Ge and Mn, which is one of driving forces of the nanocolumn formation. Furthermore, the spinodal decomposition, which is also involved in the columnar phase separation [1,7], has been substantially weakened since carbon might act as energy barrier centres during the growth of the layers. A robust argument supports this finding, may be found in a comparable structure, where only few monolayers of carbon deposited on top of the Mn_5Ge_3 greatly suppress the Mn diffusion into the adjacent Ge layer [19]. We note that we have carried out further experiments, in which we have added the same amount of carbon throughout the homoepitaxial growth of Ge on Ge substrates. When carbon is added, RHEED patterns quickly transform into three-dimensional growth mode, which can be attributed to a change of the surface energy of Ge. With data in hand, the nature and composition of these aforementioned clusters and/or disordered structures are still not clear. Probably, atom probe tomography (APT) characterizations will be needed to determine their composition and also one of the surrounding matrix.

Figure 4a displays the evolution of the temperature dependence of magnetization (M–T curves) of the samples with increase in the carbon concentration. For comparison, we also show the $M(T)$ curve of the $Ge_{0.94}Mn_{0.06}$ nanocolumn sample (without carbon). Magnetic measurements were performed by SQUID with a magnetic field of 0.5 T applied parallel to the sample surface. The film thickness is almost the same for all the samples.

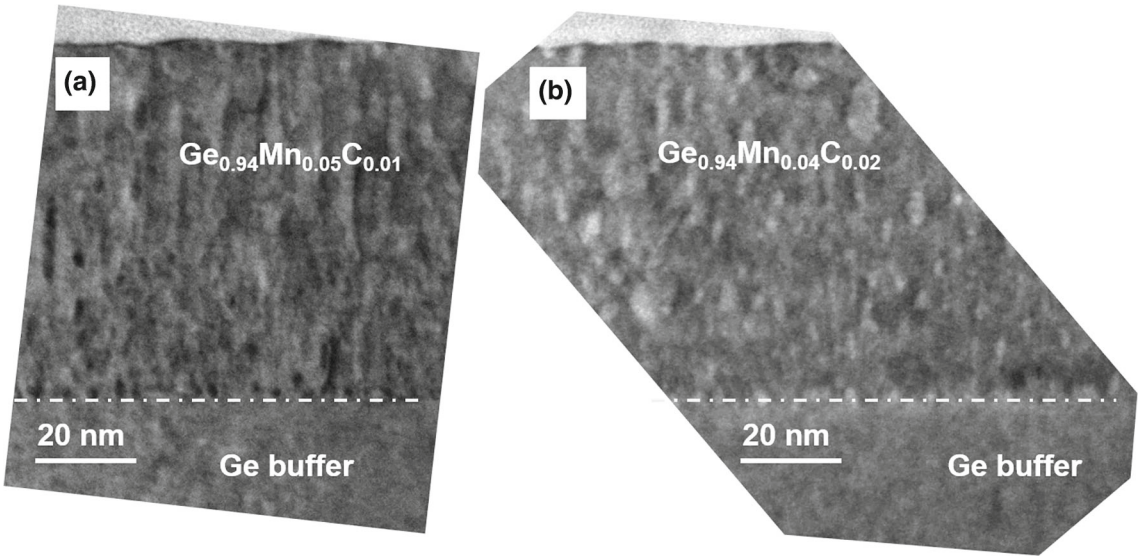

Figure 3. Typical cross-section TEM micrographs of ~80-nm-thick (**a**) $Ge_{0.94}Mn_{0.05}C_{0.01}$ and (**b**) $Ge_{0.94}Mn_{0.04}C_{0.02}$.

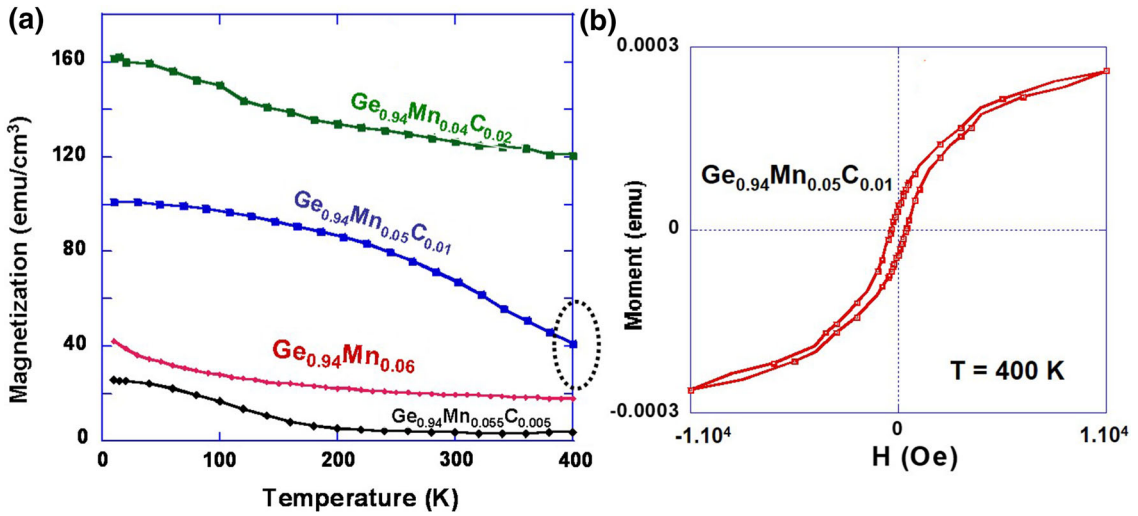

Figure 4. Evolution of magnetization *vs*. temperature of ~80-nm thick $Ge_{0.94}Mn_{0.04}C_{0.02}$, $Ge_{0.94}Mn_{0.05}C_{0.01}$, $Ge_{0.94}Mn_{0.055}C_{0.005}$ and $Ge_{0.94}Mn_{0.06}$ films (**a**) measured with a magnetic field of 0.5 T applied parallel to the sample surface; and (**b**) field-dependent magnetization loops of $Ge_{0.94}Mn_{0.05}C_{0.01}$ film with magnetic field parallel to the sample surface at 400 K.

First, it is interesting to notice that the GeMnC films contain mainly disordered nanocolumns and clusters, the ferromagnetic ordering in the samples containing carbon contents of 0.01 and 0.02 is found to persist at temperatures >400 K. To further confirm the existence of high-temperature ferromagnetism of these samples, we show in figure 4b, a measurement of field-dependent magnetization loops (hysteresis loops) of $Ge_{0.94}Mn_{0.06}C_{0.01}$ sample undertaken at 400 K. This measurement thus confirms that at 400 K, the corresponding sample still exhibits ferromagnetic behaviour. In particular, a significant increase in net magnetization is observed for carbon-doped samples as compared to the carbon-free nanocolumn sample and the magnetization increases with increasing carbon content from 0.01 to 0.02.

On the other hand, the magnetic behaviour of the sample with low carbon content (0.005) appears to be quite peculiar. The $M(T)$ curve displays a net reduction of magnetization and the Curie temperature is estimated < 200K. Note that the sample contains two layers: 20-nm thick nanocolumns and

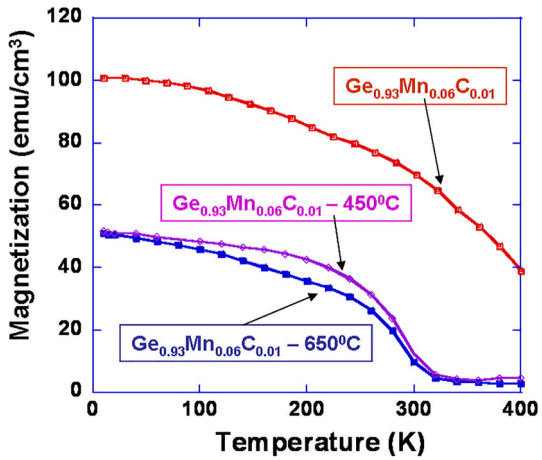

Figure 5. Evolution of magnetization *vs*. temperature of a ∼80-nm thick $Ge_{0.94}Mn_{0.05}C_{0.01}$ film after annealing at 450 and 650°C for 20 min. For comparison, magnetization of as-grown sample is shown.

60-nm thick of unknown GeMnC precipitates. Magnetic interactions *via* competing or compensative effect between the spin moments of the columnar structure and the precipitates could result in the weakness of the ferromagnetic ordering *vs.* thermal fluctuations. Further experiments in which only one layer of GeMnC and with various carbon concentrations around 0.005 should be carried out to have a comprehensive picture of this magnetic behaviour. Composition measurements should also be taken to determine the nature of GeMnC precipitates.

Preliminary study of the thermal stability of the carbon-doped MnGeC films has been conducted. Figure 5 displays the evolution of temperature-dependence magnetization of a sample with carbon content $\delta = 0.01$ upon thermal annealing at 450 and 650°C for 20 min. After annealing at 450°C, both net magnetization and the Curie temperature greatly decrease. Curie temperature of about 300 K is observed after annealing at 450 and 650°C. It is worth noting that the shape of the $M(T)$ curves obtained after annealing is very similar to that of the Mn_5Ge_3 compound [18–20]. Thus, carbon doping in this case does not allow to improve the thermal stability of the films. However, further experiments should be carried out and with various carbon concentrations to understand the role of carbon during their incorporation and annealing of MnGeC layers.

4. Conclusion

By doping carbon, we have studied the effect of carbon on the structure and magnetic properties of $Ge_{1-x}Mn_x$ nanocolumns. We have shown that carbon induces an enhancement in the magnetization and modifies the Ge–Mn growth mode. In particular, carbon reduces the diffusion coefficient of both Mn and Ge. It is also shown that GeMnC films exhibit a high Curie temperature even disordered and elongated clusters are formed instead of well-defined nanocolumns. Finally, we found a decrease of the net magnetization and the Curie temperature of the samples after annealing at 450 and 650°C. In the studied range of carbon concentrations, this finding suggests that carbon has no or a little impact in thermal stalibization against the annealing process.

Acknowledgements

We thank colleagues at Interdisciplinary Center of Nanoscience of Marseille (CINaM-CNRS), Aix-Marseille University, France, for their technical help and fruitful discussions.

References

[1] Jamet M, Barski A, Devillers T, Poydenot V, Dujardin R, Bayle-Guillemaud P *et al* 2006 *Nat. Mater.* **5** 653
[2] Li A P, Zeng C, Van Benthem K, Chisholm M F, Shen J, Rao S V S N *et al* 2007 *Phys. Rev. B* **75** R201201
[3] Zeng C, Zhang Z, van Benthem K, Chisholm M F and Weitering H H 2008 *Phys. Rev. Lett.* **100** 066101
[4] Padova P D, Ayoub J P, Berbezier I, Perfetti P, Quaresima C, Testa A M *et al* 2008 *Phys. Rev. B* **77** 045203
[5] Jaeger C, Bihler C, Vallaitis T, Goennenwein S T B, Opel M, Gross R *et al* 2006 *Phys. Rev. B* **74** 045330
[6] Van der Meulen M I, Petkov N, Morris M A, Kazakova O, Han X, Wang K L *et al* 2009 *Nano Lett.* **9** 50
[7] Devillers T, Jamet M, Barski A, Poydenot V, Bayle-Guillemaud P, Bellet-Amalric E *et al* 2007 *Phys. Rev. B* **76** 205306
[8] Le T G and Dau M T 2016 *Mod. Phys. Lett. B* **30** 1650269
[9] Le T G 2015 *Mater. Sci. Appl.* **6** 533
[10] Spiesser A, Slipukhina I, Dau M T, Arras E, Le Thanh V, Michez L *et al* 2011 *Phys. Rev. B* **84** 165203
[11] Spiesser A, Le Thanh V, Bertaina S and Michez L A 2011 *Appl. Phys. Lett.* **99** 121904
[12] Slipukhina I, Arras E, Mavropoulos Ph and Pochet P 2009 *Appl. Phys. Lett.* **94** 192505
[13] Dau M T, Le Thanh V, Le T G, Spiesser A, Petit M, Michez L A *et al* 2011 *Appl. Phys. Lett.* **99** 151908
[14] Michez L A, Spiesser A, Petit M, Bertaina S, Jacquot J F, Dufeu D *et al* 2015 *J. Phys. Condens. Matter* **27** 266001
[15] Le T G, Dau M T, Le Thanh V, Nam D N H, Petit M, Michez L A *et al* 2012 *Adv. Nat. Sci.: Nanosci. Nanotechnol.* **3** 025007
[16] Le T G, Nam D N H, Dau M T, Luong T K P, Khiem N V *et al* 2011 *J. Phys.: Conf. Ser.* **292** 012012
[17] Le T G and Nguyen Manh 2014 *J. Sci. Technol.* **52** 30
[18] Petit M, Michez L, Dutoit C E, Bertaina S, Dolocan V, Heresanu V *et al* 2015 *Thin Solid Films* **589** 427
[19] Dau M T, Le Thanh V, Le T G, Spiesser A, Petit M, Michez L *et al* 2012 *New J. Phys.* **14** 103020
[20] Dau M T, Spiesser A, Le T G, Michez L, Olive Mendez S F, Le Thanh V *et al* 2010 *Thin Solid Films* **518** S266
[21] Leifeld O 1998 *MRS Online Proceeding Library Archive* **533** 183